



# Softgrounds: substrates controlled by sediment gravity flows and the evolution of deep-water trace fossils

Yuxuan Wang<sup>1\*</sup>, Paul B. Wignall<sup>1</sup>, Jeffrey Peakall<sup>1</sup>, Jaco H. Baas<sup>2</sup> and Simon W. Poulton<sup>1</sup>

<sup>1</sup>School of Earth and Environment, University of Leeds, Leeds LS2 9JT, UK

<sup>2</sup>School of Ocean Sciences, Bangor University, Menai Bridge, Isle of Anglesey LL59 5AB, UK

 YW, 0000-0001-9266-1778; PBW, 0000-0003-0074-9129; JP, 0000-0003-3382-4578; JHB, 0000-0003-1737-5688; SWP, 0000-0001-7621-189X

\*Correspondence: [eywan@leeds.ac.uk](mailto:eywan@leeds.ac.uk)

**Abstract:** Bypassing sediment gravity flows play an important role in turbidite systems because they produce sole structures unconnected with the depositional processes of the casting bed. However, their role in facilitating seafloor colonization is underappreciated. The Aberystwyth Grits–Borth Mudstone turbidite system (Silurian, Welsh Basin) contains a famous ichnoassemblage with common graphoglyptids. This is interpreted to record colonization following erosion of surficial fluidal muds by flows that exposed firmer substrates. The burrows are developed at this level and formed beneath a thin, post-depositional mud blanket. They frequently cross-cut fluted surfaces indicating that basal turbidite bedding surfaces can record at least two, or more, bypassing flow events. Thus, even on a basin floor with thick mudstone deposition, the number of flow events will be under-represented. This Silurian turbidite system also illustrates that substrate conditions, not oxygenation, controlled trace fossil occurrence. Other than the burrows on turbidite soles, the remainder of the succession consists of thinly bedded and laminated strata typical of anoxic deposition but diverse geochemical proxies (e.g. iron speciation, trace metals) indicate full seabed oxygenation. The absence of macrofaunal bioturbation is attributed to a soft fluidal substrate in which only small-scale (meiofaunal) bioturbation is seen.

**Supplementary material:** A detailed geochemical database is available at <https://doi.org/10.6084/m9.fig-share.c.7713894>

Sedimentological substrates influence abiotic processes that generate bedforms and sole structures (e.g. Schindler *et al.* 2015; Peakall *et al.* 2020, 2024; McGowan *et al.* 2024), but they also play a role in the formation of biotic traces. However, bioturbation also changes the nature of the substrate and thus there is feedback between the two (Bromley 1990). This is particularly the case since the Cambrian owing to the increasing intensity and diversity of bioturbation (Tarhan 2018; Buatois *et al.* 2025). Thus, burrowers have greatly influenced seafloor evolution. However, the role of physical sedimentology in burrow development is also worth exploring.

The Paleozoic saw major increases in both diversity and behavioural types, initially in shallow-water settings in the Cambrian, but with sediment mixing and ichnodiversity remaining low in deeper water sediments until later in the Paleozoic (Seilacher 1977; Crimes and Crossley 1991; Crimes *et al.* 1992; Uchman and Wetzel 2011, 2012; Tarhan *et al.* 2015, 2023; Buatois *et al.* 2025). The nature of the deep-water invasion, and the reasons for its delay relative to that seen in shallow waters, has

been much debated. Measures of trace fossil diversity and behavioural complexity suggest that there was a substantial increase in the Ordovician (Crimes and Fedonkin 1994; Orr 2001; Uchman and Wetzel 2012; Buatois *et al.* 2020). Other aspects of trace fossil evolution, including the intensity of bioturbation (measured using the semi-quantitative ichnofabric index) and the thickness of the sediment mixed layer, have been used to suggest that levels typical of those encountered today had still not been achieved by the end of the Silurian (Tarhan *et al.* 2015, 2023; Tarhan 2018), a view challenged by some (Gougeon *et al.* 2018).

Other than macroevolutionary trends, there are numerous important factors that control bioturbation, including substrate type, sedimentation rate, food supply, oxygen level and turbidity (Ekdale 1985; McCann 1990; Martin 2004; Seilacher 2007; Uchman and Wetzel 2011; Wetzel and Uchman 2012; Buatois and Mángano 2013). It is unlikely that all of these parameters were constant throughout the Paleozoic, and some secular trends may have controlled the delayed colonization of the deep sea.

From: Davies, N. S. and Shillito, A. P. (eds) *Bedding Surfaces: True Substrates and Earth's Historical Archive*. Geological Society, London, Special Publications, **556**, <https://doi.org/10.1144/SP556-2025-17>

© 2025 The Author(s). This is an Open Access article distributed under the terms of the Creative Commons Attribution License (<http://creativecommons.org/licenses/by/4.0/>). Published by The Geological Society of London.

Publishing disclaimer: <https://www.lyellcollection.org/publishing-hub/publishing-ethics>

Increasing oxygen levels may have been an especially important driver (e.g. Tarhan *et al.* 2023; Buatois *et al.* 2025). Geochemical proxies have suggested that early Paleozoic oceans were poorly ventilated, and this situation only improved substantially in the Devonian (Dahl *et al.* 2010, 2019; Lu *et al.* 2018; Sperling *et al.* 2021; Haxen *et al.* 2023), although deep-sea ichnogeneric diversity increases significantly before this, in the Silurian (Buatois *et al.* 2025). There could also be a macro-evolutionary control because the specialized adaptations required for deep-sea burrowing (e.g. low levels of food availability in such settings require specialist survival strategies) may have taken millions of years to evolve (Tarhan 2018). Alternatively, the observation that many deep-sea-style trace fossils first occurred in shallow waters during the Cambrian (Crimes and Crossley 1991; Uchman and Wetzel 2011) indicates that most behavioural strategies were already established by this time. The long-term, onshore-to-offshore displacement of burrow types may have been due to more intense competition in shallower waters, driving some trace makers into deeper waters (Crimes *et al.* 1992; Orr 2001).

In order to address the factors controlling deep-sea colonization, we here describe an early Paleozoic trace fossil assemblage. The Aberystwyth Grits Group (AGG) in western Wales is a deep-water turbidite succession that accumulated in the Welsh Basin during the late Llandovery (Telychian Stage, Early Silurian) (Wood and Smith 1958; Baker and Baas 2020; Baas *et al.* 2021). It has long been celebrated for its abundant, well-preserved trace fossils on the soles of turbidite beds (Wood and Smith 1958; Crimes and Crossley 1980, 1991; McCann 1989, 1990; Orr 1995). Graphoglyptids such as *Paleodictyon* are especially abundant. Such endostratal traces are common in the deep sea today, where they may be produced by organisms that ‘farm’ bacteria in their burrow walls, thereby circumventing the problem of low food supply in oligotrophic settings (Seilacher 2007), although the ecology of *Paleodictyon* in more nutrient-rich settings is unclear (Miguez-Salas *et al.* 2023). The proportion of graphoglyptid burrow types in the Aberystwyth Grits is unusually high for the Paleozoic. The graphoglyptid ichnogenera/total ichnogenera ratio is 0.45, a value typical of Cenozoic deep-water assemblages, whereas Lower Paleozoic values are typically <0.20 (Uchman 2004; Uchman and Wetzel 2011).

In contrast, the Borth Mudstone Formation, the downdip equivalent of the Aberystwyth Grits, has no recorded trace fossils, but has well-preserved thin beds (Baker and Baas 2020), suggesting that bioturbation was inhibited by anoxia or dysoxia (McCann 1990; James 2005). In order to understand the conditions during trace fossil formation in the Aberystwyth–Borth sedimentary system,

sedimentological, geochemical and ichnological analysis of coastal outcrops has been undertaken. Here the aim is to assess the importance of factors such as redox conditions, substrate type and sediment gravity flows in controlling trace fossil development, and implications for the long-term evolution of deep-sea bioturbation.

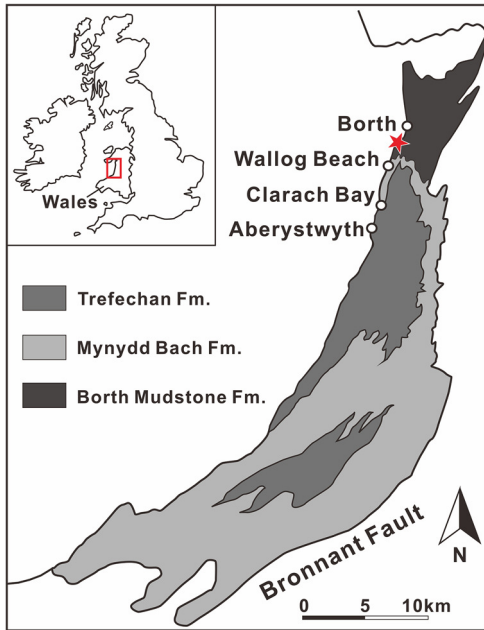
## Regional geology

Lower Silurian (Telychian Stage, Llandovery Series) strata of west Wales record a deep-water turbidite system developed within the Welsh Basin (Cherns *et al.* 2006). The turbidite system passes downdip, from SW to NE, from channelized and sheet sandstones interbedded with mudstones of the Trefechan and Mynydd Bach formations (Aberystwyth Grits Group) to the mudstone-dominated Borth Mudstone Formation (BMF) (Baker and Baas 2020). The AGG records a turbidite fan setting subject to a range of sediment gravity flows, including turbidity currents, transitional flows (*sensu* Baas *et al.* 2009), debris flows and hybrid events (Baker and Baas 2020; Baas *et al.* 2021). In contrast, the BMF is predominantly mudrock with thin beds of sandstone or siltstone (typically <1 cm thick). Deposition is suggested to have mostly occurred from turbulence-damped, mud-rich sediment gravity currents at the fan fringe (Baker and Baas 2020). As noted above, trace fossils are common and diverse on the soles of the AGG sandstone beds (Crimes and Crossley 1991), whereas no bioturbation has been reported from the BMF. Oxygen levels in the Welsh Basin during deposition are postulated to have been dysoxic (McCann 1990; Orr 1995; James 2005), with sediment gravity flows temporarily improving oxygenation levels (Orr 1995).

## Methods

The Aberystwyth Grits Group and Borth Mudstone Formation are well exposed in coastal cliffs and on wave-polished foreshore platforms to both the NE and SW of Aberystwyth. This study focuses on the cliff sections that range from north of Aberystwyth to south of Borth beach (Fig. 1). Representative sedimentary logs were measured and samples for geochemical and petrographic analysis were collected from the BMF mudstones. These included a 32.5 m-thick section in which 60 samples were collected (Fig. 2), to investigate detailed, bed-scale redox variation, and a 1.0 m thick section from which 20 samples were collected (Fig. 3). Trace fossil observations were made in the field and in thin sections and 3 dm-scale blocks were obtained for a further, high-resolution, thin-section study of the sedimentology and bioturbation. Two blocks with a

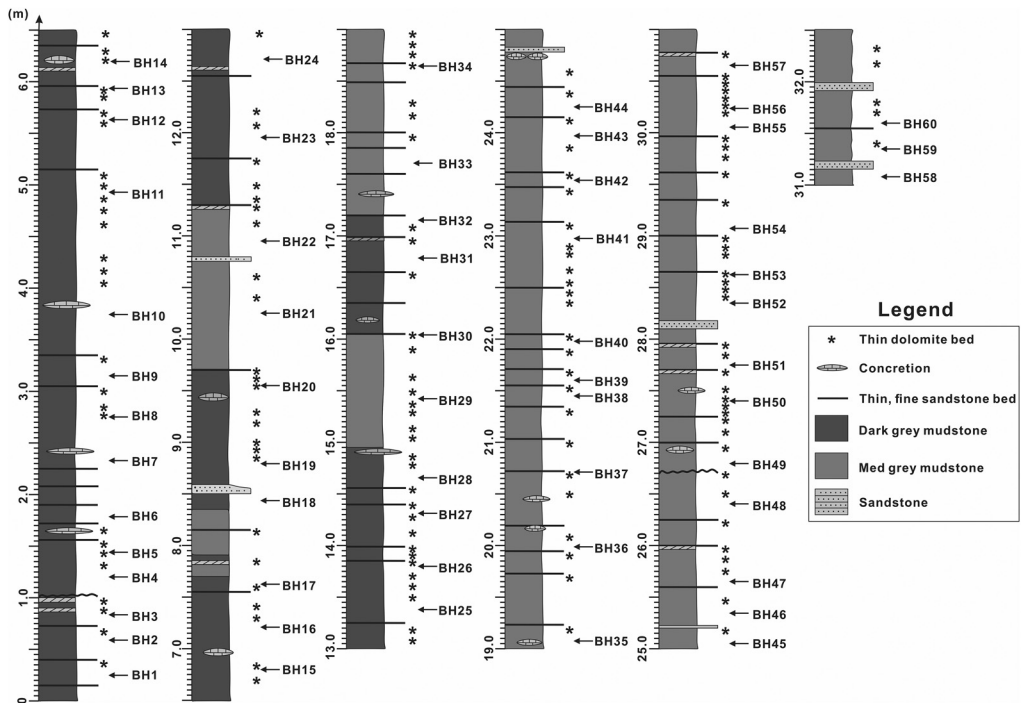
Softgrounds: gravity flows & deep-water trace fossils



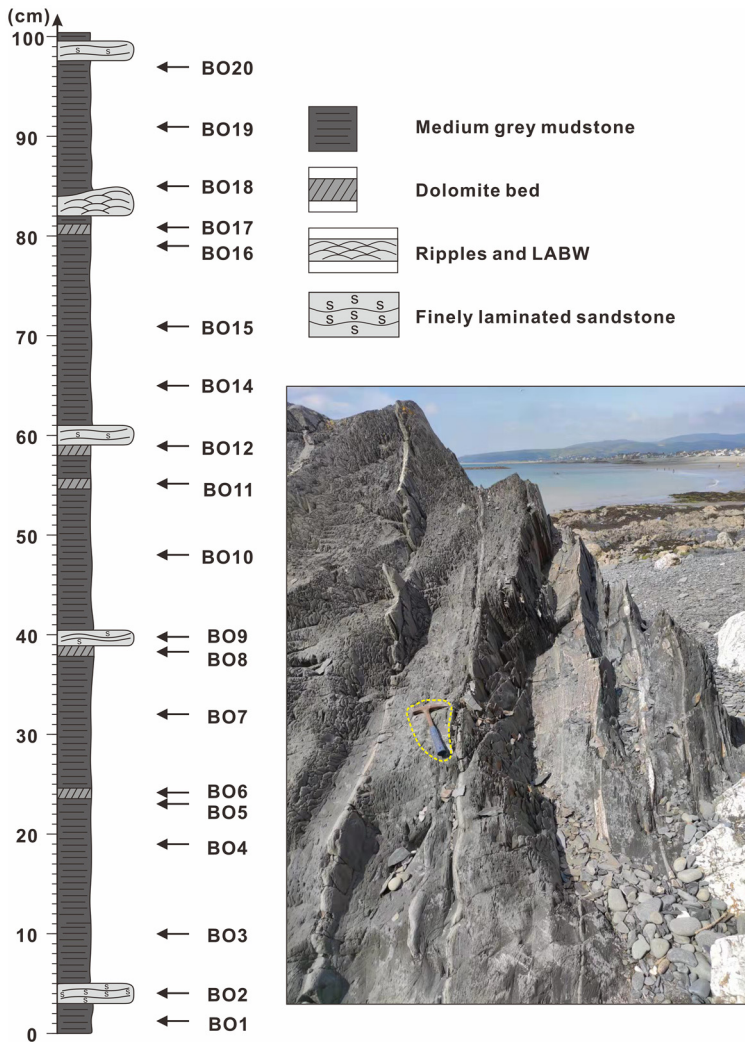
**Fig. 1.** Geological map of the Aberystwyth Grits Group and Borth Mudstone Formation in Wales. Red star represents the sampling positions. Source: modified after Baker and Baas (2020).

distinct mudstone–sandstone boundary were polished, coated in carbon and examined under a TESCAN VEGA3 scanning electron microscope (SEM) under backscatter mode. Energy dispersive spectroscopy point and area analyses were simultaneously applied to identify element distributions of single minerals and bulk surface of the SEM probe sections. Total organic carbon (TOC), iron speciation and trace and major element concentrations were analysed for all samples. Sample powders were treated with 10% HCl to remove carbonate phases prior to TOC analysis on a LECO CS-230 analyser, with an analytical precision of better than 2%. Total element concentrations were determined after ashing at 550°C for 8 h, followed by dissolution with HNO<sub>3</sub>–HF–HClO<sub>4</sub>. Samples were then dried and boric acid was added before the samples were dried again. Finally, samples were re-dissolved in hot HNO<sub>3</sub> and the major elements (Fe, Al) were determined via ICP–optical emission spectrometry, with redox sensitive trace metals (U, Mo, Re) analysed by ICP-MS. Replicate extractions of international sediment standard PACS-2 gave a relative standard deviation (RSD) of <2% for all elements, and analyses were within 3% of certified values.

Sulfide concentrations were determined via the two-step chromous chloride method (Canfield *et al.* 1986) to determine acid volatile sulfide (below



**Fig. 2.** Sedimentary log of the long section measured in the Borth Mudstone at Borth beach, showing sample horizons (BH1–BH60).

Y. Wang *et al.*

**Fig. 3.** Sedimentary log and field photograph of the high-resolution section measured in the Borth Mudstone at Borth, showing sample horizons (BO1–BO20). LABW, Low-amplitude bed wave. Hammer highlighted for scale.

detection in all cases) and pyrite concentrations. The liberated  $H_2S$  was precipitated as  $Ag_2S$  and pyrite Fe ( $Fe_{py}$ ) was determined gravimetrically. Unsulfidized Fe phases were determined via the sequential extraction scheme of Poulton and Canfield (2005). This operationally defined procedure targets Fe in carbonate phases ( $Fe_{carb}$ ), in Fe (oxyhydr)oxides ( $Fe_{ox}$ ) and in magnetite ( $Fe_{mag}$ ). Solutions from the sequential extracts were analysed via AAS, and replicate extractions of international reference material WHIT (Alcott *et al.* 2020) gave RSDs of <5% for all Fe phases.

## Results

### Sedimentology

The sedimentology of the AGG has been described in detail on several occasions (Crimes and Crossley 1980; Talling *et al.* 2004; McClelland *et al.* 2011; Baker and Baas 2020) and only a summation is presented here. More detail is presented on the less well known BMF.

Baker and Baas (2020) identified the following facies types in the AGG between Aberystwyth and

### Softgrounds: gravity flows & deep-water trace fossils

Borth (cf. Fig. 4), with the likely depositional processes given in parentheses:

- (1) massive sandstones (rapid suspension fallout from fully turbulent flow) (Fig. 4a);
- (2) laminated sandstones (suspension fallout from turbulent flow) (Fig. 4b, c);
- (3) sandstones with dispersed mudstone clasts (upper transitional plug flows *sensu* Baas *et al.* 2009);
- (4) sandstones with large current ripples (turbulence-enhanced transitional flows);
- (5) interlayered sandstone and mudstone bands and laminae (unclear origin);
- (6) siltstone, either massive or planar laminated (fine-grained turbulent flow or lower transitional plug flows);
- (7) silty mudstone in which silt grains occur ‘floating’ in the matrix (cohesive flow, preventing

settling of silt grains, as encountered in quasi-laminar plug flows);

- (8) massive mudstone, with thick developments of this facies occurring above sand and silt event beds (Fig. 4a), showing swirly textures in thin section (interpreted to have developed in the plug region of mud rich, turbulence attenuated gravity flows, cf. Baas *et al.* 2014; Stevenson *et al.* 2014); other mud horizons may record fine-grained settling after sediment gravity flow events or hemipelagic ‘background’ settling).

Sole structures are common on the base of sandstone beds and include, most commonly, flutes (Fig. 5a–d), along with grooves and more rarely chevron and skip marks (Baas *et al.* 2021). Surfaces with flute marks show a varying degree of bioturbation (described below), although non-burrowed fluted surfaces are also common.

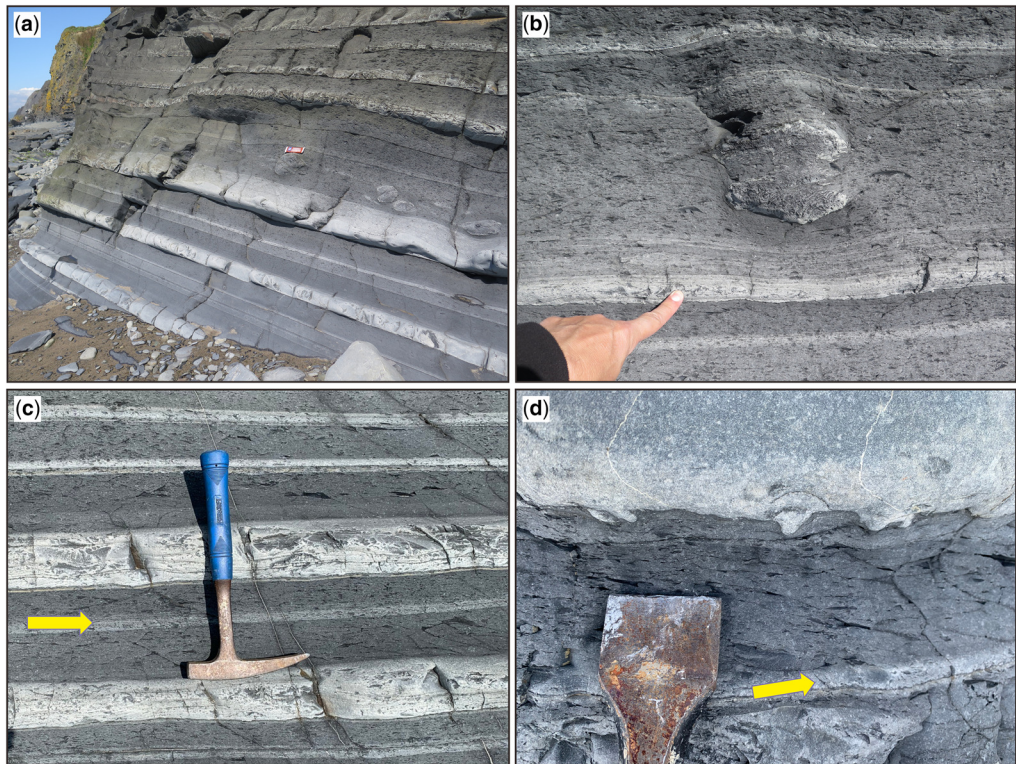


**Fig. 4.** Coastal outcrops of the Aberystwyth Grits Group. (a) Outcrop to the north of Clarach Bay, showing dominance of mudstone facies with centimetre-thick sandstone beds and several decimetre-thick beds of massive and laminated sandstone in a 4 m-thick section. (b) Finger rests on a laminated sandstone bed that passes up to interlaminated sandstone and mudstone, and then a thick mudstone bed with a concretion in its centre, north of Clarach Bay. (c) Laminated and massive sandstone beds, 2–10 cm thick, interbedded with mudstone facies that contain thin dolomite beds (yellow arrow points to one example), Wallog beach. Hammer is 30 cm long. (d) Cross-section of burrow fills in the base of a sandstone that shows faint lamination (Tb-division) that lacks burrows, north of Wallog. Yellow arrow indicates a dolomite bed in underlying mudstone. Chisel blade is 4.5 cm wide.

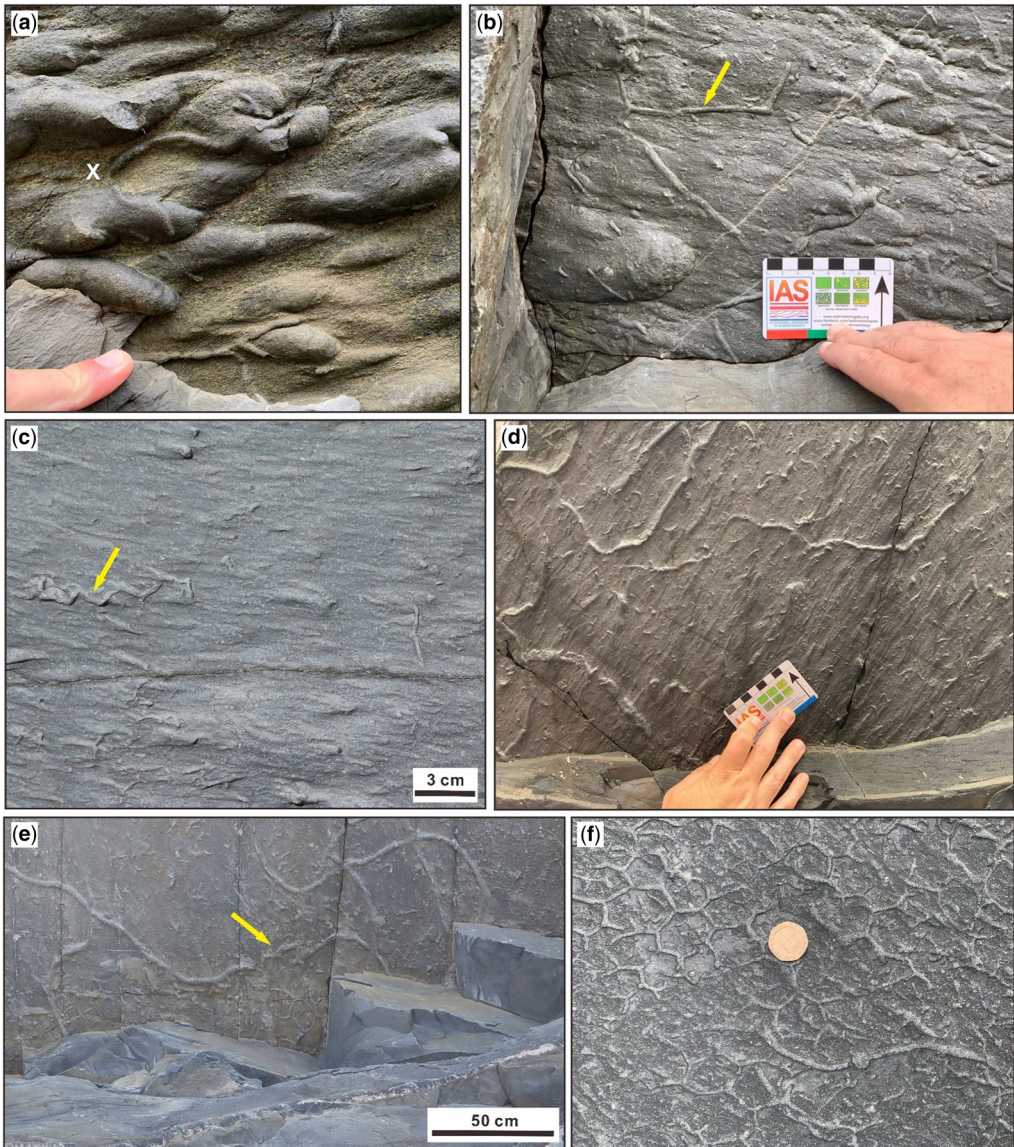


**Fig. 5.** Soles of bedding planes in the Aberystwyth Grits, all at south Wallog beach unless otherwise stated. (a) Heavily fluted surface, in which flutes are cross-cut by a *Helminthopsis* burrow. Note the gap in the burrow at x indicates a point where the trace was made in the overlying mud veneer prior to its removal by the casting turbidite. (b) Surface showing flute marks of different sizes, flow to left, cross-cut by mostly short, straight *Palaeophycus*, and a small part of a large *Paleodictyon* (arrowed). (c) Surface with small flute casts cross-cut by *Paleodictyon* (example arrowed) that are only partially preserved. North of Clarach Bay. (d) Several *Helminthopsis* cross-cutting numerous small flute and skim marks (flow towards the hand). (e) Trace-fossil assemblage, dominated by *Helminthopsis* in near full relief and faintly preserved *Paleodictyon*, suggesting the burrow networks of the latter have mostly been removed by erosion. Arrow denotes where a *Helminthopsis* burrow intersects a *Paleodictyon* and, for a short distance, follows a zig-zag path indicating that the *Paleodictyon* burrow was present first. Scale bar is approximate because the cliff overhang is inaccessible. North of Clarach Bay. (f) Surface covered in a *Paleodictyon*, cross-cut by a gently sinuous *Helminthopsis* in the lower field of view, which is in turn cross-cut by a short vertical burrow (*Bergaueria*?). Coin is 21 mm in diameter.

### Softgrounds: gravity flows & deep-water trace fossils

The BMF is dominated by variably silty mudstones that vary from dark grey to medium grey, with numerous thinner beds (typically ranging from a millimetre up to 2 cm in thickness, with a maximum of 5 cm; Talling (2001), his figure 15a) of both very dark grey and pale grey mudstones (Figs 2, 3 & 6). Silt-poor mudstones dominate much of the BMF with sparse, fine silt grains floating in the finer clay-grade matrix (the ‘starry night’ texture of Haughton *et al.* 2003). The more silt-rich levels consist of multiple, thin, silt-rich laminae alternating with clay-rich laminae (Fig. 7a, b). Silt laminae can show slightly erosive bases and are overlain by laminae composed of a mix of silt and clay-grade material (Fig. 7a). The sharp basal contacts of the silt-rich laminae show no evidence for burrowing (Fig. 7a).

In outcrop, abundant thin pale grey beds of the BMF give outcrops a distinctive ‘stripey’ appearance (Fig. 6). These beds are also present in the AGG mudstones, although less frequently (Fig. 4). In the representative 32.5 m thick section of the BMF, 149 pale grey beds were measured (Fig. 2). The composition of these layers was investigated using back-scatter SEM imagery and element mapping. This shows the mudstone to be composed of clay-grade grains of quartz, feldspar and chlorite (Fig. 8a–d). The same grain assemblage is also present in the pale grey beds but they are subordinate to abundant (>50%) dolomite rhombs around 20 µm in dimension (Fig. 8b, c). The rhombs have well-defined faces and show amalgamation and intergrowth (Fig. 8b), indicating that they are of diagenetic origin and not transported grains.

In addition to the silty mudstones (and thin dolomites), the BMF contains widely spaced thin beds (0.1–5.0 cm thick) of very fine sandstone (Figs 2 & 3). These are typically finely laminated (Fig. 9a), but the thicker beds can also show large current

ripples, wavy lamination and occasional low-amplitude bed waves (*sensu* Baker and Baas 2020). The basal contacts of the sandstone beds are sharp, sometimes slightly eroded and occasionally show small flame structures (Fig. 9b).

### Trace fossils

The celebrated trace fossil assemblages of the AGG are cast in positive hyporelief on the soles of sandstone beds that rest on mudstones. The semirelief profiles of burrows (or half relief *sensu* Crimes and Crossley 1980) are visible in cross-section (Fig. 4d), and these are the only evidence for bioturbation seen in vertical profile; the rest of the AGG (and BMF) both appear unburrowed when viewed in cliff sections (e.g. Figs 4 & 6). Sandstone beds with trace fossils at their base are typically 10–15 cm thick, although bed thicknesses range from as little as 1 cm to up to 0.5 m (Crimes and Crossley 1991). Flutes are commonly cross-cut by the trace fossils (Figs 5a–d & 10a) while grooved surfaces are not (Fig. 10b). The quality of burrow preservation also varies considerably, particularly for *Paleodictyon*, the most common burrow type. These hexagonal burrow networks are sometimes only faintly embossed (Fig. 5e), suggesting that the burrow networks were only just intersecting these surfaces and were mostly developed in an overlying mudstone, now removed. In other examples, short sections of burrows, such as the Y-shaped junctions or zig-zag lengths, are clearly preserved (Figs 5b, c, f & 10a), indicating slight variation in the burrow depth within an individual burrow network. Evidence for burrow tiering, in the form of consistent cross-cutting relationships amongst different ichnotaxa, is rare, although the meandering *Helminthopsis* are generally preserved in fuller relief and cross-cut *Paleodictyon* when they are present on the same

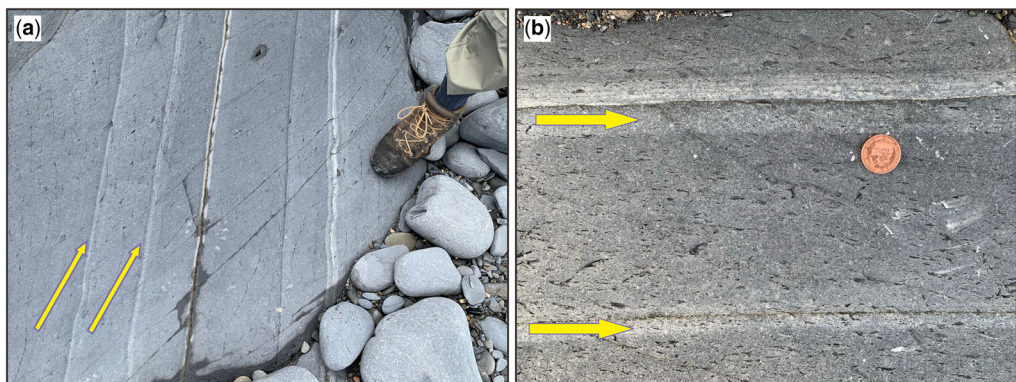


**Fig. 6.** Borth Mudstone outcrops showing dominance of mudstone with thin fine sandstone and siltstone beds and centimetre-thick beds of dolomite (arrowed). Boot for scale in (a) and 25 mm diameter coin in (b).

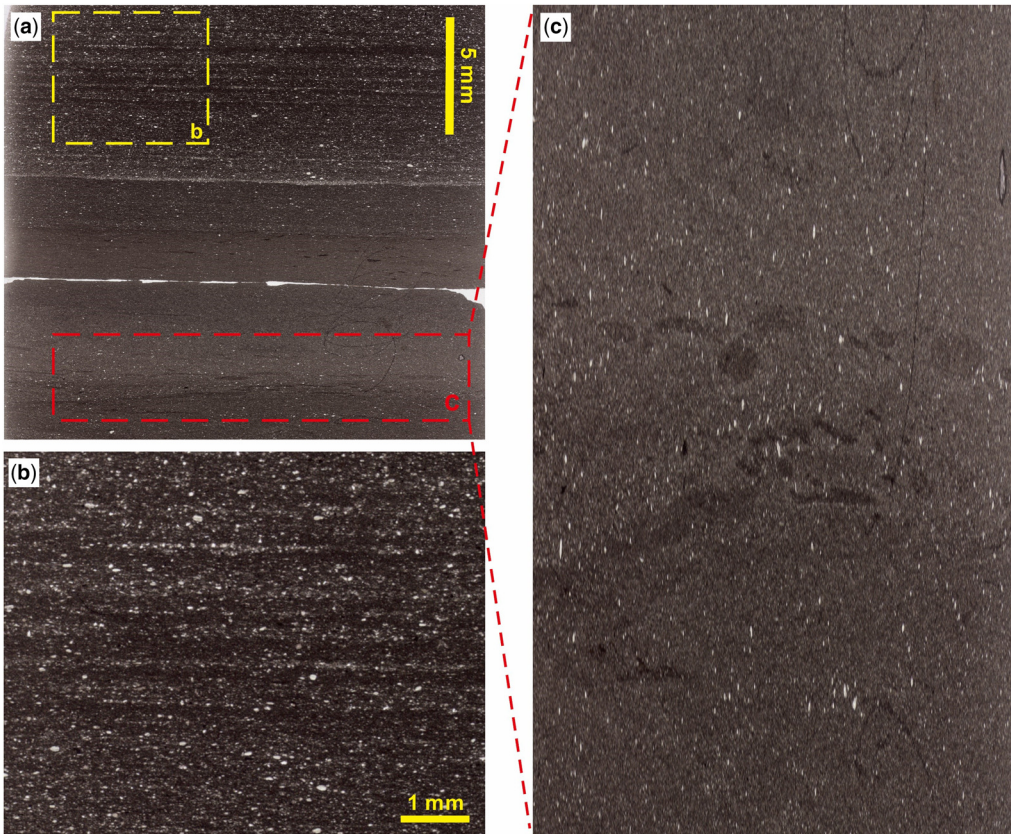


**Fig. 7.** Thin section photomicrographs of a laminated and thin-bedded sample of the Borth Mudstone. (a) Overview showing silt-poor mudstones in the lower field of view, with lamination defined by colour contrasts, and, in the upper field of view, silt-laminated mudstone. (b) Enlargement of the silt-laminated mudstone. (c) Vertically enhanced (by  $\times 10$ ) view of mudstone in (a) showing pre-compactional fabric interpreted to record meiofaunal-scale bioturbation.

surface (Fig. 5f). In rare cases, the course of *Helminthopsis* burrows may deviate where they intersect a *Paleodictyon* network (Fig. 5b). *Helminthopsis* burrows on flute-marked surfaces can show short discontinuities where the original burrow extended into the inferred overlying mudstone (see below) before returning down to the fluted surface (Fig. 5a).

Trace fossils are not discernible in the mudstones of the AGG and BMF. However, thin-section analysis reveals that there are abundant sub-millimetre-scale burrows in the silt-poor mudstone facies but not the silt-laminated mudstones (Figs 7a, c & 9a). The burrows are most clearly seen by ‘decompacting’ the sediment by vertically stretching images (Fig. 7c), which reveals that they are subhorizontal and unbranched and have blurred and diffuse boundaries. Burrowing was intense but did not extend deeper than a millimetre (compacted thickness), with the result that laminations in the silt-poor mudstones, which are defined by colour variations, have been preserved (Fig. 9a).

In summary, there are two styles of bioturbation in the AGG-BMF deep-water system: a diverse, macrofaunal burrow assemblage with common graphoglyptids restricted to the basal surfaces of sandstone turbidites, and bioturbation in the silt-poor mudstones that is more than an order of magnitude smaller. None of this bioturbation disrupts bedding, with the result that vertical profiles of the strata appear unbioturbated.

## Geochemistry

The geochemical attributes of the 32.5 and 1.0 m-thick sections are closely comparable, with neither showing any great variation amongst the different lithologies (Fig. 11). The TOC contents are low and range from 0.11 to 0.28 wt%, averaging 0.18 wt% (Fig. 11). The pale-grey dolomitized mudstones have a lower TOC content than the surrounding dark grey mudstones, often below 0.1 wt%. The iron geochemistry is similarly invariant amongst

## Softgrounds: gravity flows &amp; deep-water trace fossils

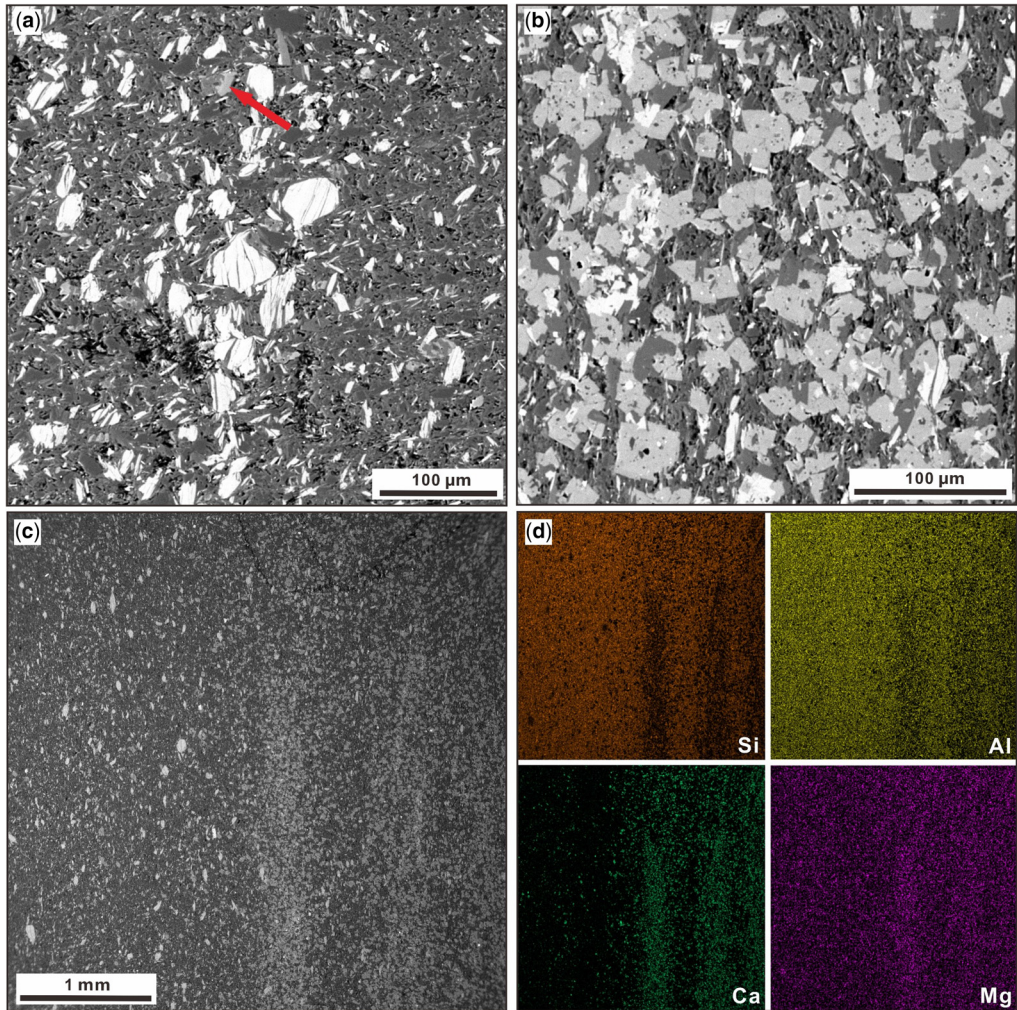


**Fig. 8.** Backscatter images of Borth Mudstone lithologies; both views have bedding near vertical. (a) Mudstone composed of chlorite (brightest grains), quartz and feldspar with rare dolomite patches (red arrow). Note the lack of other amorphous clay minerals in this mudrock. (b) Dolomite rhombs form more than half of the field of view; other grains are chlorite (bright laths), quartz (darkest grains) and feldspar. (c) Mudstone showing the vertical contact with a dolomite-rich bed in the centre of the field of view (bedding is vertical in this view). (d) Element maps of the same field of view shown in (c) in which areas with higher brightness have higher element concentrations. Dolomite-rich levels are rich in Ca and Mg, and poor in Si and Al.

samples, with very low ratios (average  $0.08 \pm 0.02$ ; Fig. 11) of highly reactive Fe ( $Fe_{HR}$ ) to total Fe ( $Fe_T$ ). The  $Fe_{HR}$  represents phases that are potentially reactive towards dissolved sulfide during deposition and diagenesis (Poulton *et al.* 2004), and the low  $Fe_{HR}/Fe_T$  values are consistently below the 0.22 threshold typical of oxic conditions (Poulton and Raiswell 2002). The  $Fe_{py}/Fe_{HR}$  ratios are also low throughout both sections, with almost no  $Fe_{py}$  present in the pale dolomitic beds (Fig. 11). The redox-sensitive trace metals, U and Mo, are generally depleted relative to

average upper continental crust ( $R_{EF}$ , 'R' stands for the reference value of trace element, and the subscript 'EF' stands for enrichment factor of each element), with average enrichment factors ( $U_{EF} = 0.64 \pm 0.05$ ,  $Mo_{EF} = 0.34 \pm 0.30$ ) supporting oxic depositional conditions at the sediment–water interface (e.g. Tribovillard *et al.* 2012). Rhenium enrichment factors (average  $1.97 \pm 0.45$ ) are only slightly enriched (Fig. 11), suggesting that the dysoxic conditions required for Re drawdown (Crusius *et al.* 1996; Morford and Emerson 1999) were restricted to sediment

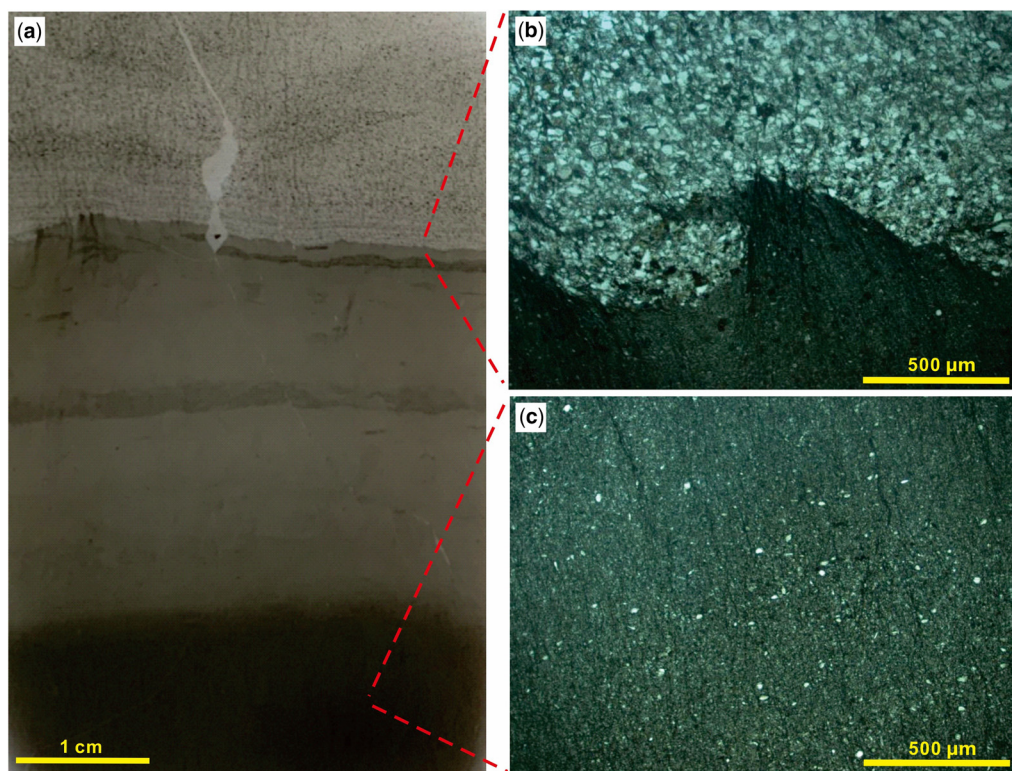


**Fig. 9.** Thin-section photomicrograph images showing sedimentary features of the Borth Mudstone. (a) Pale grey mudstone bed at centre of image overlain by a sharp (slightly erosive-based) very fine sandstone showing planar and ripple-scale cross lamination. Small-scale burrow mottling (sub-millimetre scale) can be discerned in the pale bed. The lowest part of the image shows a gradational transition to darker mudstone over a distance of *c.* 1 mm. (b) Image of the contact between the laminated fine sand and underlying pale grey mudstone showing small flame structure. (c) Image of pale grey mudstone with floating silt grains (starry night texture).

porewaters during diagenesis, which is consistent with the low TOC contents of these sediments. These combined geochemical signals suggest that the overlying water column was well oxygenated.

In summary, the lack of any enrichment in uranium means that both the sediment–water interface and the porewaters in the upper regions of the sediment profile were oxic as seen in modern environments (Morford and Emerson 1999). The lack of Mo also supports this contention and suggests that porewaters near the sediment–water interface were not sulfidic. Furthermore, this is entirely consistent with the very low total organic carbon values. There is slight enrichment in Re, which occurs under dysoxic conditions, but these are very low levels, suggesting that the porewaters became dysoxic at some depth in the sediments (Crusius *et al.* 1996; Morford *et al.* 2012). While it is impossible to precisely state what depth porewaters became dysoxic or anoxic, large enrichments in Re only occur

when the O<sub>2</sub> penetration depth is less than 1 cm into the sediment. These are not large enrichments that are reported here. The lack of any U enrichment means that porewaters were oxic to a depth at which water exchange could occur between the porewaters and the overlying water column. The multiproxy geochemical data thus provide strong lines of evidence to suggest that oxygen was not controlling the depth of bioturbation. The sediment also lacks framboidal pyrite, a typical component of dysoxic–anoxic sediments (Bond and Wignall 2010), further supporting an oxic interpretation.

## Discussion

### The nature of the substrate

The sedimentology of the AGG-BMF system records deposition in a deep-water turbidite fan setting (Crimes and Crossley 1980; Talling *et al.*

## Softgrounds: gravity flows &amp; deep-water trace fossils

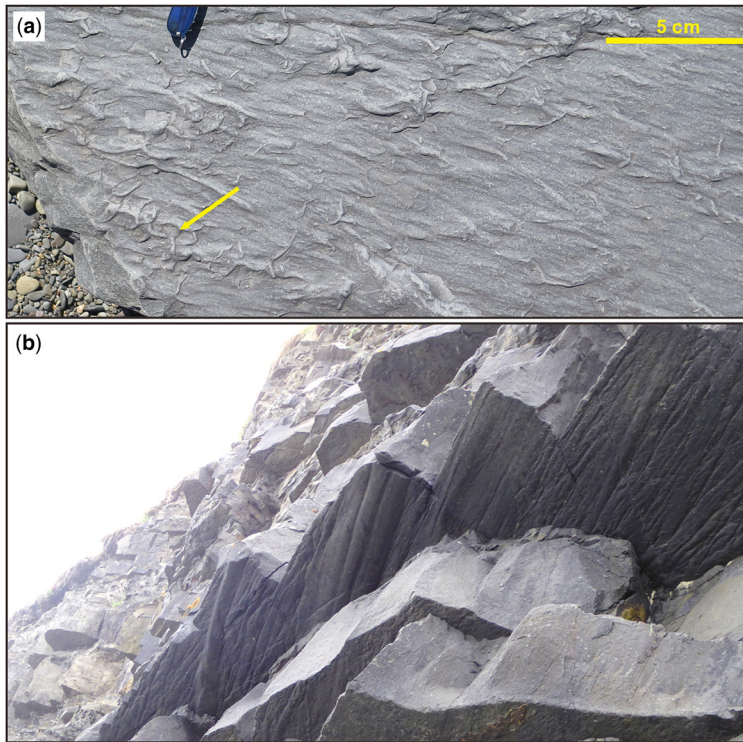


**Fig. 10.** Soles of bedding planes in the Aberystwyth Grits. (a) Surface covered in numerous small flutes indicating a flow direction to the left. Straight burrows and sections of *Paleodictyon* (example arrowed) cross-cut the flutes in numerous places. (b) Broad grooves cross-cutting longitudinal ridges and furrows (a form of flow-induced interfacial deformation structure, cf. Peakall *et al.* 2024). Note the absence of trace fossils. View is of a cliff overhang and is approximately 8 m wide.

2004; McClelland *et al.* 2011; Baker and Baas 2020), with the mudstone-dominated BMF developed on the muddy fringe of the system (Baker and Baas 2020). The dominance of mudstone with dispersed silt grains in this setting (Fig. 9c) suggests that the mud-dominated flows had sufficient cohesion to prevent particle sinking (Peakall *et al.* 2020). Such flows can be categorized broadly as ‘fluid muds’ with low yield strengths capable of supporting silt grains (Fig. 12; Talling *et al.* 2012). This categorization of ‘fluid muds’ agrees with the study of Baker and Baas (2020), who attributed the thick muds, directly above silt and sand layers, of the AGG and BMF to en-masse deposition from turbulence-attenuated, mud-rich plug flows. In contrast, the silt-laminated beds probably formed as bed load beneath a more turbulent boundary layer, indicating some variation in style from lower- to upper-transitional plug flow (Baker and Baas 2020). Despite evidence for erosive bed contacts beneath silt laminae, small mudstone rip-up clasts are not seen, even though they have been generated

in laboratory experiments on soft, watery substrates (Schieber *et al.* 2010). Such clasts typically appear as compacted lenses in ancient mudstones that show evidence for sediment transport (e.g. Schieber 2016), but their absence from the Borth Mudstone may reflect the soft nature of the seafloor substrates, an attribute that may have controlled the trace fossil occurrences, as discussed below.

### Why is bioturbation not more pervasive?

The thinly bedded and often laminated appearance of the AGG and BMF in outcrop has been used as evidence that the various styles of sediment gravity flow deposition occurred under anoxic conditions, in which even the thin beds were not disturbed by burrowing (e.g. James 2005). Furthermore, the development of abundant, thin dolomitized layers in the mudstones has not picked out any burrow networks, even though burrows are often the focus for the growth of diagenetic phases. Despite these observations, burrows are clearly present in the form of casts

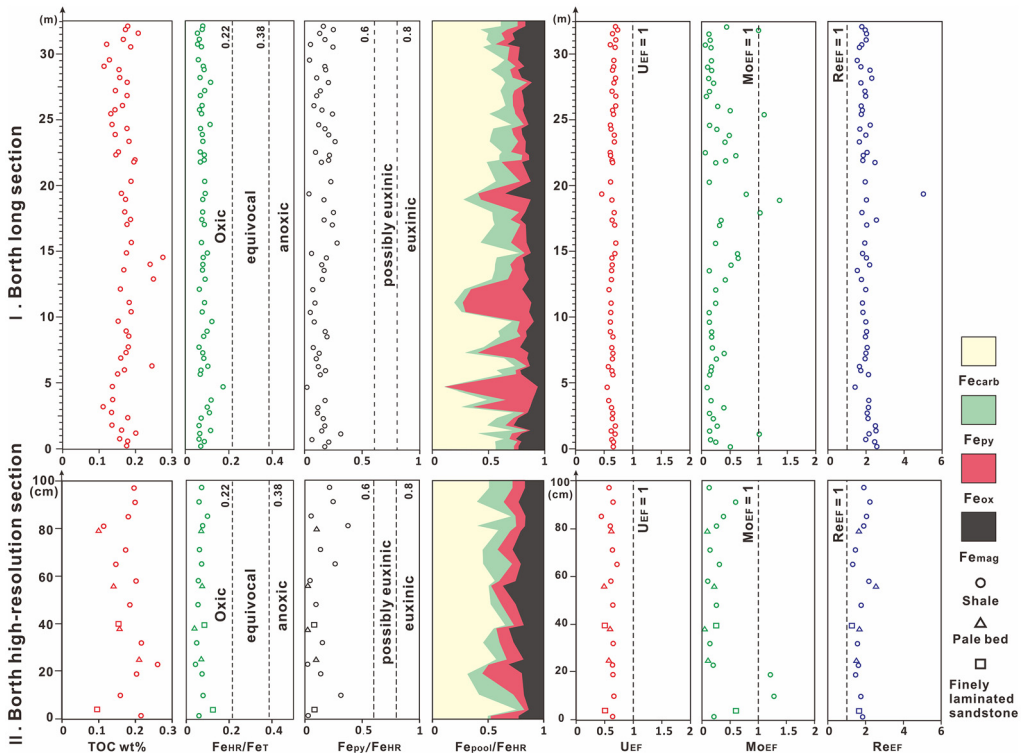


**Fig. 11.** Geochemical data for the long section, and the high-resolution section, of the Borth Mudstone Formation, Borth. Dashed lines on the plots of highly reactive Fe ( $Fe_{HR}$ ) to total Fe ( $Fe_T$ ) and pyrite Fe ( $Fe_{py}$ ) to  $Fe_{HR}$  distinguish different bottom water redox conditions (Poulton 2021), while for the enrichment factor plots, the dashed lines at a value of 1 represents the upper continental crust composition.

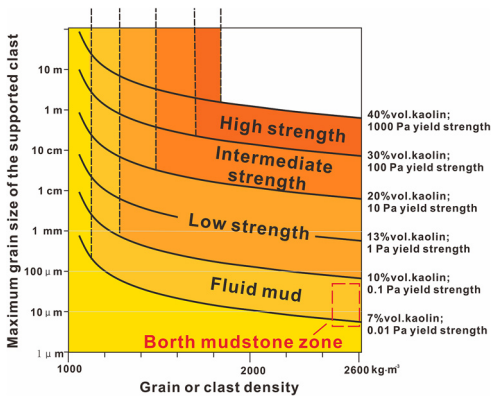


**Fig. 12.** Estimated rheology of Borth muds during deposition in a plot showing the maximum clast size that can be supported by the yield strength (matrix strength) of a mud-rich fluid, for increasing clay (kaolin) concentrations (from Talling *et al.* 2012).

on the soles of turbidites, notably those ornamented with flutes, and more pervasively, on a sub-millimetre scale in mudstones. Given the geochemical evidence from both iron speciation and trace metal concentrations for a well-oxygenated depositional setting, it is not surprising to find burrowing. Nonetheless, questions remain as to why it was not more pervasive and why there are no body fossils present, if the seabed was well oxygenated. The preservation of the trace fossils provides some clues, as discussed below.

### Preservation of trace fossils

The trace fossil assemblages, including the prominent graphoglyptids, of the AGG are cast beneath turbidite sandstones, in which the burrows were partially exhumed and eroded before being infilled by sand (Uchman and Wetzel 2012; Knaust *et al.* 2014). Reports of full-relief preservation in the AGG, either within the sandstone beds or as sand-filled burrows cast in the mudstone beds beneath (Crimes and Crossley 1980, 1991) were not

### Softgrounds: gravity flows & deep-water trace fossils

confirmed in our study. Similarly, purported faecal-pellet-filled burrows (Crimes and Crossley 1991; Orr 1995) were not seen; all trace fossils were sand filled and attached to basal surfaces of sandstones and in places had clearly been present within the overlying mudstone that was eroded prior to sandstone deposition (Fig. 5a). Modern graphoglyptids are endostratal traces that form beneath a few millimetres of surficial mud (Ekdale 1980). Therefore, the depth of erosion required to exhume the AGG traces need not have been great. However, the presence of only faint hyporelief traces (e.g. Fig. 5e) suggests that in some cases the burrows were mostly in the overlying muds, with only the basal-most part of the burrows intersecting the fluted surfaces. However, the mud blanket must have been at least a few centimetres thick in order for endostratal burrows *c.* 1 cm in diameter to form. Previous studies of the AGG have suggested that the burrows were partially eroded and cast in sand deposited by turbidity flows (Crimes and Crossley 1991; Orr 1995). This accords with their positive hyporelief preservation on the soles of turbidite sandstones, but it does not account for the fact that the burrows cross-cut sole marks, particularly flutes.

#### Process model for trace fossil development and preservation

The observation that burrows postdate the sole marks indicates that there were at least two distinct phases of erosion and sediment bypass. An initial phase of erosion of a muddy seafloor produced flutes and was followed by deposition of a thin, mud blanket, either by hemipelagic processes or by settling from the tail of the turbidity current (Fig. 13). This suggests that the turbulent or weakly transitional flows responsible for forming flutes (Peakall *et al.* 2020) bypassed their sand component down-dip. Subsequent colonization of the seabed saw burrows developed within the mud blanket at the interface between the eroded, flute-ornamented surface and its mud cap (Fig. 13). The common co-occurrence of flutes and trace fossils suggests that the rheological properties required for flutes to form in mud were optimal for the burrowers. The formative substrate conditions of flutes are poorly known; however, there must be sufficient strength to maintain relatively steep slopes at their upstream ‘noses’ (Peakall *et al.* 2020, 2024). Physical experiments on chevrons and grooves show that erosive cuts cannot be maintained in sediments with yield strengths below *c.* 70 N m<sup>-2</sup> (McGowan *et al.* 2024), equivalent to the fluid–solid category in the classification of van Rijn (1993). Consolidation times for the fluid–solid category is of the order of one year (van Rijn 1993), representing a minimum time estimate.

These estimates for yield strength are, however, based on modern clay-rich sediments (van Rijn 1993). In contrast, the muds in the BMF lack appreciable amorphous clay, instead consisting of clay-grade material composed of quartz, feldspar minerals and distinct chlorite clay grains (Fig. 8a, b). Consequently, the consolidation times of this colloidal suspension to reach equivalent yield strengths are poorly known. However, the presence of the silt grains within these muds that produces the ‘starry night’ facies, suggests that these muds exhibited strength and thus cohesion.

A second phase of erosion then followed, which removed the mud cap and deposited sand that cast the lower part of the trace fossils. This scenario requires that the second erosive event cut down precisely to the previous level of erosion, where the burrows are developed, and no deeper. The marked rheological contrast between the more-lithified older mud and the younger surficial muds may have resulted in this being a common occurrence. Trace fossils (including graphoglyptids) that cross-cut sole marks have been reported from other turbidite successions (e.g. Monaco 2008; Buatois *et al.* 2009; Monaco and Checconi 2010; Cummings and Hodgson 2011), and can be reinterpreted to record series of events similar to those shown in Figure 13. However, the bedding surfaces with burrows and sole marks only record levels that were true substrates for a short period (*sensu* Davies and Shillito 2021), because they were only briefly exposed at the seabed immediately following flute formation, and again following removal of the mud blanket, until deposition of the overlying bed. The endostratal burrows formed within a mud blanket that draped the sole structures after formation.

The AGG is famous for its bioturbation, but basal bedding surfaces lacking trace fossils are common, which may be due to a number of reasons. Firstly, the original mud cap thickness may have been too thick for burrowing organisms to have reached the sole mark surfaces. Secondly, erosion from more powerful flows may have removed the burrowed, sole-marked horizons, leaving only smooth bedding planes or a surface with only sole marks (Fig. 13). Lastly, the sole marks may have been cut by flows that then deposited a turbidite, hybrid event bed, or debrite, and associated mud-cap, on top of the surface, thus preserving the sole marks from being bioturbated. In particular, this may be the case for the rarely bioturbated, grooved surfaces that are typically overlain by debrites and hybrid event beds in the AGG (Fig. 10b; Baas *et al.* 2021). The interval between erosive episodes must have been sufficiently long to allow seafloor colonization, possibly at least several years. In modern experimental studies, colonization of the muddy deep-seafloor begins within months, although the development of diverse

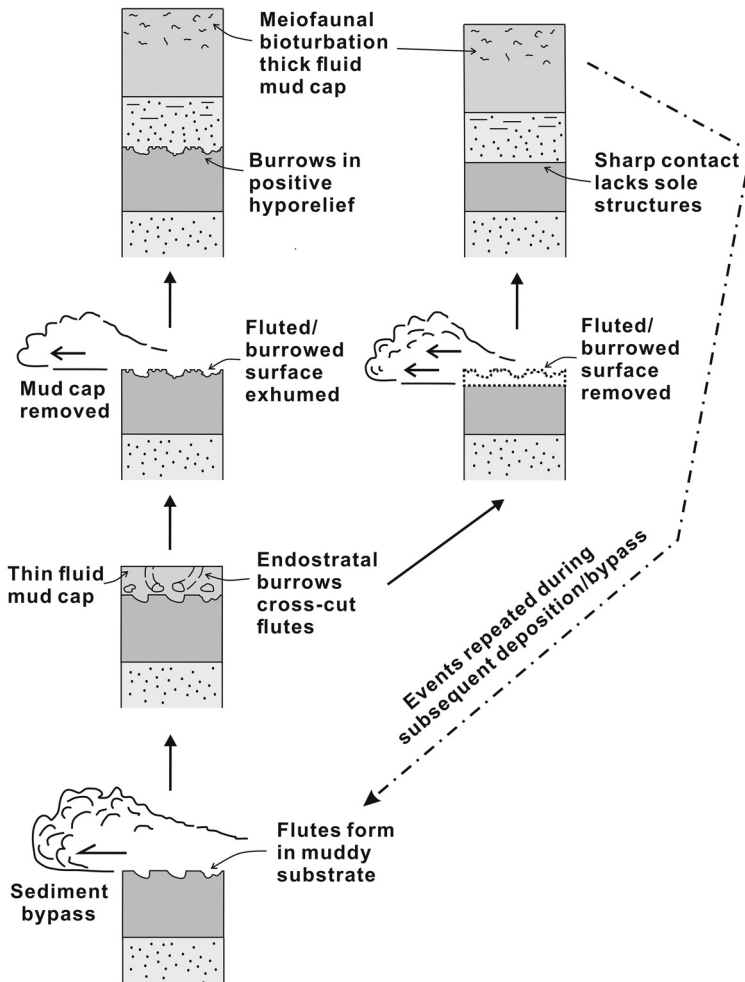


**Fig. 13.** Process models for formation of the different basal bedding surfaces seen in the sandstones of the Aberystwyth Grits Group. Note that in the case of erosion of the fluted surface, the resulting bed may show no sole structures as illustrated, or may contain grooves surfaces, or in some cases a new fluted surface (see text for details).

communities of adult organisms takes 2–5 years (Smith and Hessler 1987). Such periods of stasis are plausible for this distal part of a turbidite system, given that estimates of turbidite frequency, whilst poorly constrained, decrease down-system from *c.* 1–5 per year in canyon heads, to 1–2 per year in the mid-fan Amazon channel, to *c.* 1 per 1000 years or less in basin plain deposits (Pirmez and Imran 2003; Talling 2014). Distal submarine fan settings such as the Welsh Basin are thus in sharp contrast to early Paleozoic shallow-epieiric settings, where high sedimentation frequencies and hydrodynamic activity between depositional events consistently shorten colonization windows and thus reduce trace fossil abundance (Veenma and Davies 2025).

If macrofauna were able to colonize and burrow the muddy seafloor during AGG deposition, then why are there no endostratal burrows within the sandstones? Such burrows are present elsewhere in the Welsh Basin. For example, Orr (1995) recorded trace fossils, notably *Helminthoidea*, within contemporaneous turbidite sandstone beds developed updip from the AGG. Their absence from the AGG may relate to the greater thickness of the mud caps in the more basal location. If turbidite sands were blanketed by thick caps of fluidal mud, it would not have been possible for the larval stages of the organisms to penetrate deep enough to reach the sandy layers. By implication, the mud caps were presumably thinner in the updip locations studied by Orr

### Softgrounds: gravity flows & deep-water trace fossils

(1995), allowing some animals to burrow down into the tops of turbidite sands. In the AGG and BMF, bioturbation was restricted to the muddy layers, where it is seen (in thin section) as the tiny, diffuse burrows of meiofaunal-sized organisms (Figs 7a, c & 9a). This burrowing was insufficient to disturb even lamina-scale bedding and the resultant fabric is of a type that has been called ‘fuzzy lamination’ (Schieber and Wilson 2021). Suggestions that such fabrics are indicative of dysoxic conditions, in which larger organisms were unable to survive owing to low oxygen conditions (Schieber 2003; Schieber and Wilson 2021), are not supported by our geochemical evidence for fully oxygenated bottom water conditions. This indicates that substrate consistency is the key constraint on trace fossil development. A very soft, fluidal substrate is also likely to have ensured that shelly macrofauna were unable to settle on the muds of the AGG-BMF system. Shelly benthic organisms sink into highly fluidal muds (Wignall 1993), while soft-bodied meiofauna such as nematodes can ‘swim’ in such sediment (Moodley *et al.* 2000). Only when the fluidal mud was removed by sediment gravity currents to expose somewhat more cohesive sediment were favourable conditions for larger burrowing organisms created.

### Implications for the evolution of deep-water burrowing in the Paleozoic

The intensity and diversity of bioturbation in deep-water settings in the early Paleozoic lagged behind that of shallower-water communities (Seilacher 1977; McCann 1990; Crimes and Crossley 1991; Uchman 2004; Uchman and Wetzel 2011; Gougeon *et al.* 2018; Buatois *et al.* 2020, 2025). Various explanations have been suggested for this, including the prevalence of low-oxygen conditions in deeper waters (Haxen *et al.* 2023; Tarhan *et al.* 2023) and macroevolutionary causes such as increasing competition in shallow waters causing some groups to be displaced into deeper waters (Crimes *et al.* 1992; Orr 2001). The redox proxies from the Welsh Basin indicate fully oxygenated bottom waters, which helps explain the high diversity of the ichnoassemblages. Low-diversity trace fossil communities typical of other deep-water environments in the Early Silurian may owe their impoverishment to inhibiting factors, such as poor oxygenation. Nonetheless, the AGG trace fossils are unusual in being restricted to bedding surfaces in strata that are otherwise laminated. Graphoglyptid traces are commonly destroyed by deeper tiers of bioturbation and preserved only if exhumed and cast by eroding turbidity currents (Uchman and Wetzel 2011). Other than occasional cross-cutting (Fig. 5b), there is no

evidence for tiering of burrows in these Early Silurian basinal sediments. The AGG and BMF have a very thin ‘mixed layer’ that is less than a millimetre thick, although this thickness may have been up to a centimetre pre-compaction. It is argued here that this is because the fluidal nature of the substrate inhibited colonization by macrofauna. Only erosion by sediment gravity currents and exposure of somewhat firmer substrates facilitated the development of macrofaunal burrows.

Sediment mixed layer thicknesses – the zone of intense surficial bioturbation – are around 10 cm in modern sediments but typically only 1–2 cm in early Paleozoic sediments (Tarhan *et al.* 2015), although peak burrow depths can be greater (Mángano and Buatois 2014) and examples of well-developed mixed layers are known from shallow marine Cambrian strata (Gougeon *et al.* 2018). This increase in mixed layer thickness has been attributed to the slow rise of sediment ‘bulldozing’ by mobile deposit feeders in the Cambrian–Devonian interval (Tarhan *et al.* 2015). Our study suggests that the lack of bulldozers in our deep-water Early Silurian example was not due to oxygen limitation but to sediment fluidity. The low-clay, but clay-grade, mineral composition of the muds, and resulting colloidal suspension, probably resulted in soupy substrates in the AGG–BMF depositional system. It remains to be seen if such mud types (and their ichnofabric) are specific to this Early Silurian example, or if the lack of vegetated landscapes in the early Paleozoic ensured that there was little supply of clay minerals to the oceans (McMahon and Davies 2018). In such conditions, it was the nature of the sediment gravity flows that was the key control on trace fossil development. Ideal conditions occurred when erosion exposed partly lithified muds of suitable consistency for traces to develop, although a thin blanket of fluidal mud was also required for the endostratal organisms to thrive.

### Implications for classification of trace fossils

Trace fossils in turbiditic successions are frequently categorized as pre-depositional (e.g. graphoglyptids) and post-depositional (e.g. Seilacher 1962; Cabrera-Ortiz *et al.* 2025; Uchman and Wetzel 2025). However, the present work shows that where there are fluted surfaces such characterization can be misleading. In the present examples, the graphoglyptids are post-depositional with the original mud-blanket deposited above the fluted surfaces; however, they are pre-depositional relative to the bed that ultimately sits above the fluted surfaces. Even more complex erosion-and-deposition histories can be inferred from some published examples of fluted surfaces. For example, figure 6c of Buatois *et al.* (2009) shows small flutes, cross-cut by burrows, before a

second set of larger flutes was formed which are also cross-cut by a later generation of burrows. At least three distinct flows must have been involved in the generation of such surfaces. The terms pre- and post-depositional thus do not work in examples where there are significant periods of coarse-grained bypass, followed by stasis and subsequent re-excitation of surfaces. We recommend that the terms such as hypichnial and endichnial are utilized to describe traces because they do not infer the timing *a priori*.

### Implications for deep-water systems: sedimentation v. bypass

The importance of sediment bypass during deposition of the AGG indicates that sediment gravity flows were more common than a simple count of the preserved bed number indicates. Fluted surfaces cross-cut by burrows record at least two discrete events with a period of considerable stasis (probably several years) between flows (Fig. 13). They could also record multiple repetitions of such events with most episodes going unrecorded. The burrowed surfaces record highly fortuitous conditions during deposition from the final flow, and even unornamented basal surfaces could record many events (the right-hand option in Fig. 13 could be repeated many times). The implication is that assessment of event frequency may be impossible even in a basin-floor submarine fan system, rendering calculations of such criteria (e.g. Talling 2001; Sylvester 2007; Marini *et al.* 2016) problematic. In particular, the bypass of sands appears strongly related to the turbulent to lower transitional plug flows (*sensu* Baas *et al.* 2009) that formed fluted surfaces (Peakall *et al.* 2020). These missing sands may in part explain the observation of a prominent break in the thickness distributions of turbiditic sandstones, between high-concentration, and low-concentration turbidites (e.g. Rothman and Grotzinger 1995; Talling 2001; Sylvester 2007). The evidence for bypass of sands in turbulent dominated flows may also apply to the transition between the products of high- and low-concentration turbidity currents (HDTC v. LDTC), and if so may provide a putative answer for the rarity of complete Bouma sequences (with a full set of divisions A–E). The hypothetical model of Allen (1985, his figure 12.25; reproduced in Bridge and Demicco (2008) and Leeder (2011)) for the longitudinal distribution of the Bouma divisions has the divisions stacking progressively downstream. However, this still leaves a considerable zone where complete Bouma sequences would be expected. Bypass of the fluidal low-concentration turbidity currents suggests an enhanced mobility of flows at this point, and thus the  $T_{cde}$  divisions may be significantly

offset downdip relative to the  $T_{ab}$  divisions. Presumably this offset is sufficient to make the probability of complete Bouma sequences very low. Likewise, the vertical deposition rate in turbidites is often assumed to progressively decrease upwards (Allen 1991, his figure 1; Stow *et al.* 1996; Collinson and Mountney 2019). In contrast, the enhanced mobility of low-concentration flows suggests that there should be a marked reduction in deposition rate or even a hiatus at the HDTC to LDTC divide (e.g. Sumner *et al.* 2008); in turn followed by a reduced deposition rate in the  $T_{cde}$  divisions as shown in the experiments of Sumner *et al.* (2008) and see also Talling (2001) and Sylvester (2007).

### Conclusions

The AGG and BMF record two distinct styles of bioturbation: trace fossil assemblages on the soles of turbidites and meiofaunal (sub-millimetre scale) burrows in mudstones. The former traces are almost always found cross-cutting flutes, but only rarely on grooved surfaces. The burrowed surfaces record at least two distinct flow events. Initial flute formation by a bypassing sediment gravity current was followed by deposition of a thin mud blanket. Trace fossils formed at the flute surface/mud blanket interface over the ensuing few years before a second flow event re-exhumed the fluted surface and cast both the flutes and trace fossils (in positive hyporelief) at the base of turbidite sand. The frequent description of such basal-turbidite trace fossils as ‘pre-depositional’ is inappropriate because the surface on which they occur has a history of both erosion and deposition. In contrast, grooved surfaces showed only temporary stasis (insufficient for colonization and burrowing) between the formation of the grooves by the debritic head of the flow (Baas *et al.* 2021) and the deposition of an overlying coarse bed. Consequently, bypass of the coarse-grained component of some types of sediment gravity flow is key to the formation and preservation of the traces in the AGG. The trace fossils indicate that the bypass of turbidites that form flutes is relatively common in the AGG (and probably in other turbidite systems too). Previous work has suggested that there could be marked periods of stasis between sole structures and the overlying deposit, and that this should be accommodated in a revised Bouma sequence (Peakall *et al.* 2020; Baas *et al.* 2021). Here we provide evidence for this process and highlight that it is most common at fluted surfaces.

Macrofaunal-scale burrowing is not seen in the mudstones. These are thinly bedded and composed of clay-grade detrital grains (quartz, feldspar, chlorite) with ‘floating’ silt grains interpreted to indicate deposition from a cohesive flow of fluid mud.

## Softgrounds: gravity flows & deep-water trace fossils

Geochemical proxies (Fe speciation and fluctuations of the redox-sensitive trace metals U, Mo and Re), combined with the absence of pyrite framboids, indicate that seafloor conditions were fully oxygenated during mudstone deposition. Numerous, centimetric pale brown beds are shown to be formed from diagenetic dolomite. The absence of visible bioturbation is attributed to the soupy nature of the muddy substrates that probably impeded seafloor colonization, except for meiofaunal organisms that were able to ‘swim’ through the substrate producing diffuse burrows and fuzzy lamination. It was only the exhumation of firmer substrates by sediment gravity flows that allowed larger organisms to colonize. Claims that fuzzy lamination is indicative of dysoxic conditions inimical to macrofaunal life are not supported by the geochemical proxies. Substrate consistency was therefore the paramount control on trace fossil development in the Early Silurian Welsh Basin, with the degree of erosion by sediment gravity flows being the main variable. Contemporaneous (and older) deep-water trace fossil assemblages are generally less diverse than the AGG assemblages. The normal oxygenation levels may have facilitated the elevated diversity seen in our study, a conclusion that indirectly supports the idea that the colonization and bioturbation of many or most deep-water early Paleozoic settings was impeded by poor oxygenation of deeper waters at this time (Dahl *et al.* 2010, 2019; Lu *et al.* 2018; Sperling *et al.* 2021; Haxen *et al.* 2023). Nonetheless, our study shows that using sedimentary criteria alone for redox levels, such as the preservation of fine lamination, is not reliable unless supported by combined geochemical and petrographic evidence.

**Acknowledgements** We thank two anonymous reviewers, and editor Neil Davies for their comments on the present manuscript. We also thank Gabriela Mángano, Luis Buatois and Alfred Uchman for comments on an earlier version of this manuscript.

**Competing interests** The authors declare that they have no known competing financial interests or personal relationships that could have appeared to influence the work reported in this paper.

**Author contributions** YW: data curation (equal), methodology (equal), visualization (lead), writing – original draft (lead), writing – review & editing (supporting); PBW: conceptualization (lead), methodology (equal), supervision (lead), writing – review & editing (lead); JP: conceptualization (equal), investigation (equal), writing – review & editing (supporting); JHB: investigation (supporting), writing – review & editing (supporting); SWP: methodology (lead), supervision (lead), writing – review & editing (supporting).

**Funding** This study was funded by a University of Leeds research training grant (YW) and Natural Environment Research Council grant NE/T008458/1 (SWP). JHB’s visit to the field sites was funded by Equinor.

**Data availability** All data generated or analysed during this study are included in this published article (and, if present, its supplementary information files).

## References

- Alcott, L.J., Krause, A.J. *et al.* 2020. Development of iron speciation reference materials for palaeoredox analysis. *Geostandards and Geoanalytical Research*, **44**, 581–591, <https://doi.org/10.1111/ggr.12342>
- Allen, J.R.L. 1985. *Principles of Physical Sedimentology*. Allen and Unwin, London.
- Allen, J.R.L. 1991. The Bouma division A and the possible duration of turbidity currents. *Journal of Sedimentary Petrology*, **61**, 291–295.
- Baas, J.H., Best, J.L., Peakall, J. and Wang, M. 2009. A phase diagram for turbulent, transitional, and laminar clay suspension flows. *Journal of Sedimentary Research*, **79**, 162–183, <https://doi.org/10.2110/jsr.2009.025>
- Baas, J.H., Manica, R., Puhl, E., Verhagen, I. and Borges, A.L.D.O. 2014. Processes and products of turbidity currents entering soft muddy substrates. *Geology*, **42**, 371–374, <https://doi.org/10.1130/G35296.1>
- Baas, J.H., Tracey, N.D. and Peakall, J. 2021. Sole marks reveal deep-marine depositional process and environment: implications for flow transformation and hybrid-event-bed models. *Journal of Sedimentary Research*, **91**, 986–1009, <https://doi.org/10.2110/jsr.2020.104>
- Baker, M.L. and Baas, J.H. 2020. Mixed sand–mud bedforms produced by transient turbulent flows in the fringe of submarine fans: indicators of flow transformation. *Sedimentology*, **67**, 2645–2671, <https://doi.org/10.1111/sed.12714>
- Bond, D.P.G. and Wignall, P.B. 2010. Pyrite framboid study of marine Permian–Triassic sections: a complex anoxic event and its relationship to contemporaneous mass extinction. *Bulletin of the Geological Society of America*, **122**, 1265–1279, <https://doi.org/10.1130/B30042.1>
- Bridge, J.S. and Demicco, R.V. 2008. *Earth Surface Processes, Landforms and Sediment Deposits*. Cambridge University Press, Cambridge.
- Bromley, R.G. 1990. *Trace Fossils: Biology and Taphonomy*. Unwin and Hyman, London.
- Buatois, L.A. and Mángano, M.G. 2013. Ichnodiversity and ichnodisparity: significance and caveats. *Lethaia*, **46**, 281–292, <https://doi.org/10.1111/let.12018>
- Buatois, L.A., Mángano, M.G., Brussa, E.D., Benedetto, J.L. and Pompei, J.F. 2009. The changing face of the deep: colonization of the Early Ordovician deep-sea floor, Puna, northwest Argentina. *Palaeogeography, Palaeoclimatology, Palaeoecology*, **280**, 291–299, <https://doi.org/10.1016/j.palaeo.2009.06.014>
- Buatois, L.A., Mángano, M.G., Minter, N.J., Zhou, K., Wisshak, M., Wilson, M.A. and Olea, R.A. 2020.

- Quantifying ecospace utilization and ecosystem engineering during the early Phanerozoic – the role of bioturbation and bioerosion. *Science Advances*, **6**, eabb0618, <https://doi.org/10.1126/sciadv.abb0618>
- Buatois, L.A., Mángano, M.G., Paz, M., Minter, N.J. and Zhou, K. 2025. Early colonization of the deep-sea bottom – the protracted build-up of an ecosystem. *Proceedings of the National Academy of Science*, **122**, e2414752122, <https://doi.org/10.1073/pnas.2414752122>
- Cabrera-Ortiz, J.F., Dorador, J., Rodríguez-Tovar, F.J. and Pérez-Asensio, J.N. 2025. Paleoenvironmental conditions and evolution of a muddy turbidite system: an integrated sedimentological and ichnological analysis. *Journal of Sedimentary Research*, **95**, 86–103, <https://doi.org/10.2110/jsr.2024.101>
- Canfield, D.E., Raiswell, R., Westrich, J.T., Reaves, C.M. and Berner, R.A. 1986. The use of chromium reduction in the analysis of reduced inorganic sulfur in sediments and shales. *Chemical Geology*, **54**, 149–155, [https://doi.org/10.1016/0009-2541\(86\)90078-1](https://doi.org/10.1016/0009-2541(86)90078-1)
- Cherns, L., Cocks, L., Davies, J., Hillier, R., Waters, R. and Williams, M. 2006. Silurian: the influence of extensional tectonics and sea-level changes on sedimentation in the Welsh Basin and on the Midland Platform. *Geological Society, London, Special Publications*, **63**, 75–102, <https://doi.org/10.1144/GOEWP.4>
- Collinson, J. and Mountney, N. 2019. *Sedimentary Structures*, 4th edn. Dunedin Academic Press, Edinburgh, Scotland.
- Crimes, T.P. and Crossley, J. 1980. Inter-turbidite bottom current orientation from trace fossils with an example from the Silurian flysch of Wales. *Journal of Sedimentary Research*, **50**, 821–830.
- Crimes, T.P. and Crossley, J. 1991. A diverse ichnofauna from Silurian flysch of the Aberystwyth Grits Formation, Wales. *Geological Journal*, **26**, 27–64, <https://doi.org/10.1002/gj.3350260104>
- Crimes, T.P. and Fedonkin, M.A. 1994. Evolution and dispersal of deepsea traces. *Palaios*, **9**, 74–83, <https://doi.org/10.2307/3515080>
- Crimes, T.P., Hidalgo, J.G. and Poire, D. 1992. Trace fossils from Arenig flysch sediments of Eire and their bearing on the early colonisation of the deep seas. *Ichnos*, **2**, 61–77, <https://doi.org/10.1080/10420949209380076>
- Crusius, J., Calvert, S., Pedersen, T. and Sage, D. 1996. Rhenium and molybdenum enrichments in sediments as indicators of oxic, suboxic and sulfidic conditions of deposition. *Earth and Planetary Science Letters*, **145**, 65–78, [https://doi.org/10.1016/S0012-821X\(96\)00204-X](https://doi.org/10.1016/S0012-821X(96)00204-X)
- Cummings, J.P. and Hodgson, D.M. 2011. Assessing controls on the distribution of ichnotaxa in submarine fan environments, the Basque Basin, Northern Spain. *Sedimentary Geology*, **239**, 162–187, <https://doi.org/10.1016/j.sedgeo.2011.06.009>
- Dahl, T.W., Connelly, J.N. *et al.* 2019. Atmosphere–ocean oxygen and productivity dynamics during early animal radiations. *Proceedings of the National Academy of Science*, **116**, 19352–19361, <https://doi.org/10.1073/pnas.1901178116>
- Dahl, T.W., Hammarlund, E.U. *et al.* 2010. Devonian rise in atmospheric oxygen correlated to the radiations of terrestrial plants and large predatory fish. *Proceedings of the National Academy of Science*, **107**, 17911–17915, <https://doi.org/10.1073/pnas.1011287107>
- Davies, N.S. and Shillito, A.P. 2021. True substrates: the exceptional resolution and unexceptional preservation of deep time snapshots on bedding surfaces. *Sedimentology*, **68**, 3307–3356, <https://doi.org/10.1111/sed.12900>
- Ekdale, A. 1980. Graphoglyptid burrows in modern deep-sea sediment. *Science*, **207**, 304–306, <https://doi.org/10.1126/science.207.4428.304>
- Ekdale, A. 1985. Paleocology of the marine endobenthos. *Palaeogeography, Palaeoclimatology, Palaeoecology*, **50**, 63–81, [https://doi.org/10.1016/S0031-0182\(85\)80006-7](https://doi.org/10.1016/S0031-0182(85)80006-7)
- Gougeon, R.C., Mangano, M.G., Buatois, L.A., Narbonne, G.M. and Laing, B.A. 2018. Early Cambrian origin of the shelf sediment mixed layer. *Nature Communications*, **9**, 1909, <https://doi.org/10.1038/s41467-018-04311-8>
- Houghton, P.D., Barker, S.P. and McCaffrey, W.D. 2003. ‘Linked’debrites in sand-rich turbidite systems – origin and significance. *Sedimentology*, **50**, 459–482, <https://doi.org/10.1046/j.1365-3091.2003.00560.x>
- Haxen, E.R., Schovsbo, N.H. *et al.* 2023. ‘Hypoxic’ Silurian oceans suggest early animals thrived in a low-O<sub>2</sub> world. *Earth and Planetary Science Letters*, **622**, 118416, <https://doi.org/10.1016/j.epsl.2023.118416>
- James, D.M.D. 2005. Palaeotopography of the northern portion of the Telychian (Silurian) turbidite basin in central Wales. *Geological Journal*, **40**, 593–601, <https://doi.org/10.1002/gj.1028>
- Knaust, D., Warchol, M. and Kane, I.A. 2014. Ichnodiversity and ichnoabundance: revealing depositional trends in a confined turbidite system. *Sedimentology*, **61**, 2218–2267, <https://doi.org/10.1111/sed.12134>
- Leeder, M. 2011. *Sedimentology and Sedimentary Basins: From Turbulence to Tectonics*. Wiley-Blackwell, Oxford.
- Lu, W., Ridgwell, A. *et al.* 2018. Late inception of a resiliently oxygenated upper ocean. *Science*, **361**, 174–177, <https://doi.org/10.1126/science.aar5372>
- Mángano, M.G. and Buatois, L.A. 2014. Decoupling of body-plan diversification and ecological structuring during the Ediacaran–Cambrian transition: evolutionary and geobiological feedbacks. *Proceedings of the Royal Society B*, **281**, 20140038, <https://doi.org/10.1098/rspb.2014.0038>
- Marini, M., Patacci, M., Felletti, F. and McCaffrey, W. 2016. Fill to spill stratigraphic evolution of a confined turbidite mini-basin succession, and its likely well bore expression: the Castagnola Fm, NW Italy. *Marine and Petroleum Geology*, **69**, 94–111, <https://doi.org/10.1016/j.marpetgeo.2015.10.014>
- Martin, K.D. 2004. A re-evaluation of the relationship between trace fossils and dysoxia. *Geological Society, London, Special Publications*, **228**, 141–156, <https://doi.org/10.1144/GSL.SP.2004.228.01.08>
- McCann, T. 1989. The ichnogenus *Desmograpton* from the Silurian of Wales – first record from the Paleozoic. *Journal of Paleontology*, **63**, 950–953, <https://doi.org/10.1017/S0022336000036696>
- McCann, T. 1990. Distribution of Ordovician–Silurian ichnofossil assemblages in Wales – implications for

## Softgrounds: gravity flows &amp; deep-water trace fossils

- Phanerozoic ichnofaunas. *Lethaia*, **23**, 243–255, <https://doi.org/10.1111/j.1502-3931.1990.tb01451.x>
- McClelland, H., Woodcock, N. and Gladstone, C. 2011. Eye and sheath folds in turbidite convolute lamination: Aberystwyth Grits Group, Wales. *Journal of Structural Geology*, **33**, 1140–1147, <https://doi.org/10.1016/j.jsg.2011.05.007>
- McGowan, D., Salián, A., Baas, J.H., Peakall, J. and Best, J. 2024. On the origin of chevron marks and striated grooves, and their use in predicting mud bed rheology. *Sedimentology*, **71**, 687–708, <https://doi.org/10.1111/sed.13148>
- McMahon, W.J. and Davies, N.S. 2018. Evolution of alluvial mudrock forced by early land plants. *Science*, **359**, 1022–1024, <https://doi.org/10.1126/science.aan4660>
- Miguez-Salas, O., Rodríguez-Tovar, F.J., Ekdale, A.A., Kaiser, S., Brandt, A. and Gooday, A.J. 2023. Northernmost (Subarctic) and deepest record of Paleodictyon: paleoecological and biological implications. *Scientific Reports*, **13**, 7181, <https://doi.org/10.1038/s41598-023-34050-w>
- Monaco, P. 2008. Taphonomic features of *Paleodictyon* and other grapholyptid trace fossils in Oligo-Miocene thin-bedded turbidites, northern Apennines, Italy. *Palaios*, **23**, 667–682, <https://doi.org/10.2110/palo.2007.p07-016r>
- Monaco, P. and Checconi, A. 2010. Taphonomic aspects of the Miocene ichnofossil *Lagerstätte* from calcarenite turbiditic beds in the Verghereto Marls Formation (Northern Apennines, Italy). *Rivista Italiana di Paleontologia e Stratigrafia*, **116**, 237–252.
- Moodley, L., Chen, G., Heip, C. and Vincx, M. 2000. Vertical distribution of meiofauna in sediments from contrasting sites in the Adriatic Sea: clues to the role of abiotic v. biotic control. *Ophelia*, **53**, 203–212, <https://doi.org/10.1080/00785326.2000.10409450>
- Morford, J.L. and Emerson, S. 1999. The geochemistry of redox sensitive trace metals in sediments. *Geochimica Cosmochimica Acta*, **63**, 1735–1750, [https://doi.org/10.1016/S0016-7037\(99\)00126-X](https://doi.org/10.1016/S0016-7037(99)00126-X)
- Morford, J.L., Martin, W.R. and Carney, C.M. 2012. Rhenium geochemical cycling: insights from continental margins. *Chemical Geology*, **324**, 73–86, <https://doi.org/10.1016/j.chemgeo.2011.12.014>
- Orr, P.J. 1995. A deep-marine ichnofaunal assemblage from Llandovery strata of the Welsh Basin, west Wales, UK. *Geological Magazine*, **132**, 267–285, <https://doi.org/10.1017/S0016756800013601>
- Orr, P.J. 2001. Colonization of the deep-marine environment during the early Phanerozoic: the ichnofaunal record. *Geological Journal*, **36**, 265–278, <https://doi.org/10.1002/gj.891>
- Peakall, J., Best, J. *et al.* 2020. An integrated process-based model of flutes and tool marks in deep-water environments: implications for palaeohydraulics, the Bouma sequence and hybrid event beds. *Sedimentology*, **67**, 1601–1666, <https://doi.org/10.1111/sed.12727>
- Peakall, J., Best, J., Baas, J.H., Wignall, P.B., Hodgson, D.M. and Łapcik, P. 2024. Flow-induced interfacial deformation structures (FIDS): implications for the interpretation of palaeocurrents, flow dynamics and substrate rheology. *Sedimentology*, **71**, 1709–1743, <https://doi.org/10.1111/sed.13219>
- Pirmez, C. and Imran, J. 2003. Reconstruction of turbidity currents in Amazon Channel. *Marine and Petroleum Geology*, **20**, 823–849, <https://doi.org/10.1016/j.marpetgeo.2003.03.005>
- Poulton, S.W. 2021. The iron speciation paleoredox proxy. In: Lyons, T., Turchyn, A. and Reinhard, C. (eds) *Elements in Geochemical Tracers in Earth System Science*. Cambridge University Press.
- Poulton, S.W. and Canfield, D.E. 2005. Development of a sequential extraction procedure for iron: implications for iron partitioning in continentally derived particulates. *Chemical Geology*, **214**, 209–221, <https://doi.org/10.1016/j.chemgeo.2004.09.003>
- Poulton, S.W. and Raiswell, R. 2002. The low-temperature geochemical cycle of iron: from continental fluxes to marine sediment deposition. *American Journal of Science*, **302**, 774–805, <https://doi.org/10.2475/ajs.302.9.774>
- Poulton, S.W., Krom, M.D. and Raiswell, R. 2004. A revised scheme for the reactivity of iron (oxyhydr) oxide minerals towards dissolved sulfide. *Geochimica Cosmochimica Acta*, **68**, 3703–3715, <https://doi.org/10.1016/j.gca.2004.03.012>
- Rothman, D.H. and Grotzinger, J.P. 1995. Scaling properties of gravity-driven sediments. *Nonlinear Processes in Geophysics*, **2**, 178–185, <https://doi.org/10.5194/npg-2-178-1995>
- Schieber, J. 2003. Simple gifts and buried treasures – implications of finding bioturbation and erosion surfaces in black shales. *The Sedimentary Record*, **1**, 4–8, <https://doi.org/10.2110/sedred.2003.2.4>
- Schieber, J. 2016. Mud re-distribution in epicontinental basins – exploring likely processes. *Marine and Petroleum Geology*, **71**, 119–133, <https://doi.org/10.1016/j.marpetgeo.2015.12.014>
- Schieber, J. and Wilson, R.D. 2021. Burrows without a trace – how meioturbation affects rock fabrics and leaves a record of meiobenthos activity in shales and mudstones. *PalZ*, **95**, 767–791, <https://doi.org/10.1007/s12542-021-00590-7>
- Schieber, J., Southard, J.B. and Schimmelmann, A. 2010. Lenticular shale fabrics resulting from intermittent erosion of water-rich muds – interpreting the rock record in the light of recent flume experiments. *Journal of Sedimentary Research*, **80**, 119–128, <https://doi.org/10.2110/jsr.2010.005>
- Schindler, R.J., Parsons, D.R. *et al.* 2015. Sticky stuff: redefining bedform prediction in modern and ancient environments. *Geology*, **43**, 399–402, <https://doi.org/10.1130/G36262.1>
- Seilacher, A. 1962. Paleontological studies of turbidite sedimentation and erosion. *Journal of Geology*, **70**, 227–234 <https://doi.org/10.1086/626811>
- Seilacher, A. 1977. Evolution of trace fossil communities. *Developments in Palaeontology and Stratigraphy*, **5**, 359–376, [https://doi.org/10.1016/S0920-5446\(08\)70331-5](https://doi.org/10.1016/S0920-5446(08)70331-5)
- Seilacher, A. 2007. Principles of ichnostratigraphy. SEPM, Special Publications, **88**, 53–56.
- Smith, C.R. and Hessler, R.R. 1987. Colonization and succession in deep-sea ecosystems. *Trends in Ecology and Evolution*, **2**, 359–363, [https://doi.org/10.1016/0169-5347\(87\)90136-4](https://doi.org/10.1016/0169-5347(87)90136-4)
- Sperling, E.A., Melchin, M.J. *et al.* 2021. A long-term record of early to mid-Paleozoic marine redox change.

- Science Advances*, **7**, eabf4382, <https://doi.org/10.1126/sciadv.abf4382>
- Stevenson, C.J., Talling, P.J., Masson, D.G., Sumner, E.J., Frenz, M. and Wynn, R.B. 2014. The spatial and temporal distribution of grain-size breaks in turbidites. *Sedimentology*, **61**, 1120–1156, <https://doi.org/10.1111/sed.12091>
- Stow, D.A.V., Reading, H.G. and Collinson, J. 1996. Deep seas. In: Reading, H.G. (ed.) *Sedimentary Environments and Facies*, 3rd edn. Blackwell, Oxford, 380–442.
- Sumner, E.J., Amy, L.A. and Talling, P.J. 2008. Deposit structure and processes of sand deposition from decelerating sediment suspensions. *Journal of Sedimentary Research*, **78**, 529–547, <https://doi.org/10.2110/jsr.2008.062>
- Sylvester, Z. 2007. Turbidite bed thickness distributions: methods and pitfalls of analysis and modelling. *Sedimentology*, **54**, 847–870, <https://doi.org/10.1111/j.1365-3091.2007.00863.x>
- Talling, P.J. 2001. On the frequency distribution of turbidite thickness. *Sedimentology*, **48**, 1297–1329, <https://doi.org/10.1046/j.1365-3091.2001.00423.x>
- Talling, P.J. 2014. On the triggers, resulting flow types and frequencies of subaqueous sediment density flows in different settings. *Marine Geology*, **352**, 155–182, <https://doi.org/10.1016/j.margeo.2014.02.006>
- Talling, P.J., Amy, L.A., Wynn, R.B., Peakall, J. and Robinson, M. 2004. Beds comprising debrite sandwiched within co-genetic turbidite: origin and widespread occurrence in distal depositional environments. *Sedimentology*, **51**, 163–194, <https://doi.org/10.1111/j.1365-3091.2004.00617.x>
- Talling, P.J., Masson, D.G., Sumner, E.J. and Malgesini, G. 2012. Subaqueous sediment density flows: depositional processes and deposit types. *Sedimentology*, **59**, 1937–2003, <https://doi.org/10.1111/j.1365-3091.2012.01353.x>
- Tarhan, L.G. 2018. The early Paleozoic development of bioturbation – evolutionary and geobiological consequences. *Earth-Science Reviews*, **178**, 177–207, <https://doi.org/10.1016/j.earscirev.2018.01.011>
- Tarhan, L.G., Droser, M.L., Planavsky, N.J. and Johnston, D.T. 2015. Protracted development of bioturbation through the early Palaeozoic era. *Nature Geosciences*, **8**, 865–869, <https://doi.org/10.1038/ngeo2537>
- Tarhan, L.G., Nolan, R.Z., Westacott, S., Shaw, J.O. and Pruss, S.B. 2023. Environmental and temporal patterns in bioturbation in the Cambrian–Ordovician of Western Newfoundland. *Geobiology*, **21**, 571–591, <https://doi.org/10.1111/gbi.12560>
- Tribovillard, N., Algeo, T.J., Baudin, F. and Riboulleau, A. 2012. Analysis of marine environmental conditions based on molybdenum–uranium covariation – applications to Mesozoic paleoceanography. *Chemical Geology*, **324–325**, 46–58, <https://doi.org/10.1016/j.chemgeo.2011.09.009>
- Uchman, A. 2004. Phanerozoic history of deep-sea trace fossils. *Geological Society, London, Special Publications*, **228**, 125–139, <https://doi.org/10.1144/GSL.SP.2004.228.01.07>
- Uchman, A. and Wetzel, A. 2011. Deep-sea ichnology: the relationships between depositional environment and endobenthic organisms. In: Hüneke, H. and Mulder, T. (eds) *Deep-Sea Sediments, Developments in Sedimentology*. Elsevier, **63**, 517–556.
- Uchman, A. and Wetzel, A. 2012. Deep-sea fans. In: Knaust, D. and Richard, G.B. (eds) *Trace Fossils as Indicators of Sedimentary Environments, Developments in Sedimentology*. Elsevier, **64**, 643–671.
- Uchman, A. and Wetzel, A. 2025. Are there ‘true substrates’ in turbidite depositional settings? *Geological Society, London, Special Publications*, **556**, <https://doi.org/10.1144/SP556-2024-132>
- Van Rijn, L.C. 1993. *Principles of Sediment Transport in Rivers, Estuaries and Coastal Seas*. Amsterdam, Aqua Publications.
- Veenma, Y.P. and Davies, N.S. 2025. Short-stasis signatures in Cambrian and Ordovician shallow-marine sandstones: implications for the ichnological record and time preserved at outcrop. *Geological Society, London, Special Publications*, **556**, <https://doi.org/10.1144/SP556-2024-96>
- Wetzel, A. and Uchman, A. 2012. Hemipelagic and pelagic basin plains. In: Knaust, D. and Richard, G.B. (eds) *Trace Fossils as Indicators of Sedimentary Environments, Developments in Sedimentology*. Elsevier, **64**, 673–701.
- Wignall, P.B. 1993. Distinguishing between oxygen and substrate control in fossil benthic assemblages. *Journal of the Geological Society, London*, **150**, 193–196, <https://doi.org/10.1144/gsjgs.150.1.0193>
- Wood, P.A. and Smith, A.J. 1958. The sedimentation and sedimentary history of the Aberystwyth Grits (Upper Llandoveryan). *Quarterly Journal of the Geological Society*, **114**, 163–195, <https://doi.org/10.1144/gsjgs.114.1.0163>